Reactive and Functional Polymers 109 (2016) 42–51

Contents lists available at ScienceDirect

Reactive and Functional Polymers

journal homepage: www.elsevier.com/locate/react

Preparation and fracture process of high strength hyaluronic acid hydrogels cross-linked by ethylene glycol diglycidyl ether

Burak Tavsanli, Oguz Okay *

Istanbul Technical University, Department of Chemistry, 34469 Istanbul, Turkey

ARTICLE INFO

Article history:
Received 21 June 2016
Received in revised form 4 October 2016
Accepted 4 October 2016
Available online 06 October 2016

Keywords:
Hyaluronic acid
Hydrogels
Cross-linking
Double-network
Fracture process

ABSTRACT

We present a synthetic strategy to produce high-strength hydrogels based on hyaluronic acid, a unique biomacromolecule with distinctive biological functions. The hydrogels were prepared using a two-step procedure. In the first step, hyaluronic acid (HA) was chemically cross-linked in aqueous solutions using ethylene glycol diglycidyl ether (EGDE) under various experimental conditions. EGDE-cross-linked HA hydrogels containing 97–99% water were fragile, and ruptured when compressed to 25–51% strain under 0.02–0.15 MPa stresses. By applying the double-network approach in the second step, we were able to generate high strength HA/poly(*N*,*N*-dimethylacrylamide) double-network hydrogels containing 84–94% water. Tuning the ratio of the network components could result in hydrogels exhibiting a compressive modulus of 0.9 MPa that sustain 19.4 MPa compressive stresses, which are much larger than those reported before for the hydrogels derived from the methacrylated HA macromers. Thus, the hydrogels presented here are promising materials to make use the characteristics of HA in stress-bearing biomedical applications. Cyclic mechanical tests show irreversible stress-strain curves with a large hysteresis indicating that elastically effective cross-links of HA first-network are irreversibly destroyed under load by dissipating energy. This internal fracture of HA network together with the high mass ratio of the second to the first-network components are responsible for the extraordinary mechanical properties of the hydrogels.

1. Introduction

Hyaluronic acid (HA) is a natural anionic polyelectrolyte consisting of disaccharide repeat units of β-1,4-D-glucuronic acid - β-1,3-*N*-acetyl-D-glucosamine [1]. HA is the main component of extracellular matrix, and it plays an important role in wound-healing processes [2]. Because of the distinctive biological functions and lubricating properties, HA is an effective biomaterial for soft tissue regeneration [3–6]. However, rapid in vivo degradation and poor biomechanical performance of pure native HA limit its clinical applications. To generate a less degradable HA with improved mechanical properties, HA was chemically cross-linked to form HA hydrogels [7,8]. The functional groups in HA as potential cross-link points are the one carboxyl group and four hydroxyl groups on its repeat unit, which can be cross-linked via ester and ether linkages, respectively (Scheme 1).

Cross-linking of HA has been reported using several cross-linkers [9–15], including divinyl sulfone (DVS), glutaraldehyde (GTA), 1-ethyl-3-(3-dimethylaminopropyl) carbodiimide (EDC), ethylene glycol diglycidyl ether (EGDE), butanediol diglycidyl ether (BDDE) and poly(ethylene glycol) diglycidyl ether (PEGDE). Although the cross-linking of HA reduces its degradation rate and solubility in aqueous media, the resulting hydrogels exhibit poor mechanical properties to be used in stress-bearing applications. The lack of mechanical strength in HA hydrogels is mainly due to the absence of a viscoelastic dissipation in the chemically cross-linked HA network leading to the fracture of the hydrogels under low stresses [16,17]. Recently, high-toughness HA hydrogels with a macroporous structure have been prepared using cryogelation of aqueous HA solutions at subzero temperatures in the presence of EGDE cross-linker [18,19]. Due to the cryoconcentration of the reactants in the unfrozen micro-domains of the cryogelation system [20], HA cryogels are very tough and can completely be squeezed without any crack propagation. However, the toughness of HA cryogels is due to water flowing out of their macropores under stress and, they are very soft materials exhibiting an elastic modulus of below 2 kPa [18].

An alternative two-step approach to produce HA hydrogels is the chemical modification of HA prior to the cross-linking reactions to incorporate additional functional groups. The widely used strategy is to introduce photopolymerizable methacrylate groups on HA molecules using glycidyl methacrylate, which are subsequently photopolymerized to form HA-based hydrogels [21–23]. Another strategy is the synthesis of thiol-functionalized HA which spontaneously forms intermolecular disulfide bonds upon exposure to air [24,25]. To increase the rate of cross-linking, Michael-type addition reaction was also employed by

---

* Corresponding author.
E-mail address: okayo@itu.edu.tr (O. Okay).

http://dx.doi.org/10.1016/j.reactfunctpolym.2016.10.001
1381-5148/© 2016 Elsevier B.V. All rights reserved.

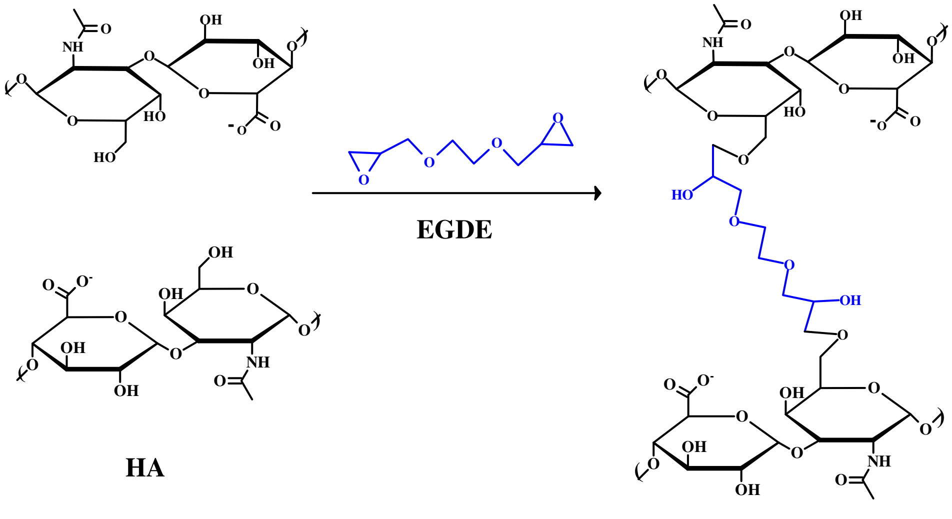

Scheme 1. Cross-linking of hyaluronic acid (HA) using ethylene glycol diglycidyl ether (EGDE).

the addition of poly(ethylene glycol) diacrylate cross-linker [24]. However, the hydrogels derived from the chemically modified HA also exhibit poor mechanical properties [26,27]. To achieve a high mechanical strength, they can be reinforced with other macromolecules [28–30], or energy dissipation mechanisms can be created to slow crack propagation within the gel network [31,32]. By using the double-network (DN) concept [33–37], Weng et al. prepared mechanically strong HA hydrogels consisting of a highly cross-linked methacrylated HA (GMHA) first-network and a lightly cross-linked ductile poly(*N*,*N*-dimethylacrylamide) (PDMA) second-network [31]. DN hydrogels exhibit a compressive modulus of 0.5 MPa and a fracture stress of 5.2 MPa. A similar procedure was recently applied by Tavsanli et al. for the synthesis of triple-network hydrogels [32]. The hydrogels consisting of GMHA/PDMA/PDMA interconnected interpenetrated network components exhibit compressive fracture stresses up to 20 MPa.

However, the chemical modification procedures of HA summarized above to prepare DN hydrogels involve macromonomer synthesis and purification steps with many chemicals including dihydrazides, trimethylamine and phase transfer catalysts. Alternatively, a simple way to produce DN hydrogels is to use native HA to create the first-network hydrogels instead of GMHA. Moreover, because GMHA is more hydrophobic than HA due to its methacrylate groups, one may expect that the single-network HA hydrogels will exhibit a higher degree of swelling in aqueous solutions as compared to GMHA hydrogels. This means that a larger amount of the second ductile PDMA network component could be introduced in HA hydrogels during double networking leading to better mechanical properties [33]. This is the main motivation of this study.

Here, we use pure native HA for the preparation of mechanically strong double-network HA hydrogels. To our knowledge, such hydrogels have not been reported before. HA hydrogels were prepared in aqueous HA solutions in the presence of EGDE cross-linker under various experimental conditions. EGDE contains epoxide groups on both ends and, has been widely used for cross-linking of biopolymers carrying hydroxyl, amino, and sulfhydryl groups [38–40]. Since the hydroxyl groups on HA molecules react with the EGDE [18,19], intermolecular cross-links form during gelation, resulting in the formation of a three-dimensional HA network (Scheme 1). We monitored the cross-linking reactions of HA with EGDE cross-linker in alkaline solutions by rheometry using oscillatory deformation tests. HA hydrogels formed were subjected to rheological and mechanical measurements to evaluate their viscoelastic and mechanical properties as a function of the cross-linker content. By applying DN approach, we were able to generate HA/PDMA hydrogels containing 84–94% water. The hydrogels sustain 0.8–19.4 MPa compressive stresses and exhibit compressive moduli up to 0.9 MPa. These values are much larger than those reported before for DN hydrogels derived from GMHA macromers [31,32]. Thus, HA hydrogels described here are promising materials for stress-bearing biomedical applications. As will be discussed below, high mechanical strength of the present hydrogels is due to the internal fracture of HA network by dissipating energy as well as due to the larger swelling capacity of the first-network hydrogels based on HA as compared to GMHA, increasing the ratio of the second-to-first network components in DN hydrogels.

2. Materials and methods

2.1. Materials

Hyaluronic acid sodium salt (HA) from Streptococcus equi was obtained from Sigma-Aldrich (impurities: ≤1 protein), and its viscosity averaged molecular weight is 1.2×10^6 g·mol^{-1} [18]. Ethylene glycol diglycidyl ether (EGDE, Polysciences, Inc., total chlorine content: 0.6%), NaOH (Merck, ≥99%), *N*,*N*-dimethylacrylamide (DMA, Sigma-Aldrich, 99%, contains 500 ppm monomethyl ether hydroquinone as inhibitor), 2-oxoglutaric acid (Fluka, ≥99%), and N,N -methylene(bis)acrylamide (BAAm, Merck, ≥99%), were used as received.

2.2. Hydrogel preparation

HA solutions were prepared by dissolving HA in 1 w/v% NaOH solution by gently stirring at 25 °C for 1 h. To ensure a complete dissolution, HA solutions were kept at 4 °C for 24 h. After adding EGDE cross-linker, the solution was stirred for 15 min before being transferred into plastic syringes (inner diameter = 6 mm, length = 70 mm) to conduct the cross-linking reactions. The reactions were carried out both at 25 °C and 50 °C for 4 days and 4 h, respectively. DN hydrogels were synthesized by immersing HA hydrogels in as-prepared states in aqueous solutions containing the monomer DMA (30 w/v%), the second-network cross-linker BAAm (0.05 and 0.10 mol% of DMA), and the photo-initiator 2-oxoglutaric acid (0.1 mol% of DMA). The volume of the aqueous solution was much larger than the gel volume (around 120 mL solution per gram of hydrogel sample), so that the concentration of the solution was practically unchanged. After the swelling equilibrium was established within 4 days, the solution containing the hydrogel was transferred into syringes of 10 mL in volume and the polymerization was carried out 25 °C under UV light at 365 nm for 24 h.

2.3. Swelling and gel fraction measurements

Hydrogel samples in as-prepared states were immersed in a large excess of water at 25 °C for at least 4 days whereby the water was replaced every day to extract any soluble species. The swelling equilibrium was tested by weighing the gel specimens. The hydrogels in both as-prepared and equilibrium swollen states were transparent indicating that macrophase separation did not occur. The equilibrium relative weight swelling ratio m_{rel} was calculated as $m_{rel} = m/m_o$, where m is the mass of the equilibrium swollen gel sample, and m_o is its mass after preparation. To determine the gel fraction, the equilibrium swollen gel samples were taken out of water and immersed into excess acetone for 1 day. After drying at 80 °C under vacuum to constant mass, the gel fraction W_g was calculated from the masses of dry polymer network and from the comonomer feed.

2.4. Rheological experiments

The cross-linking reactions of HA with EGDE cross-linker were monitored at 50 °C within the rheometer (Gemini 150 Rheometer system, Bohlin Instruments) equipped with a cone-and-plate geometry (cone angle = 4°, diameter = 40 mm). The instrument was equipped with a Peltier device for temperature control. During the rheological measurements, a solvent trap was used and the outside of the upper plate was covered with a thin layer of low-viscosity silicone oil to prevent the evaporation of water. An angular frequency ω of 6.3 rad s^{-1} and a deformation amplitude γ_o of 0.01 were selected to ensure that the oscillatory deformation is within the linear regime. After a reaction time of 3 h, the elastic moduli G' of the reaction solutions approached limiting values. Then, frequency-sweep tests were carried out at 25 °C.

2.5. Mechanical tests

Uniaxial compression measurements were conducted on equilibrium swollen hydrogels at 25 °C on a Zwick Roell Z0.5 TH test machine using a 500 N load cell. The gel samples were cut into cubic samples with dimensions 3 × 3 × 3 mm. Before the test, an initial compressive contact of 0.01 N was applied to ensure a complete contact between the gel and the plates. The tests were performed at a constant cross-head speed of 0.3 and 1 mm $\min^{-1}$ below and above 15% compression, respectively. Compressive stress was presented by its nominal σ_{nom} and true values σ_{true} ($=\lambda\ \sigma_{nom}$), which are the forces per cross-sectional area of the undeformed and deformed gel specimen, respectively, and λ is the deformation ratio (deformed length/initial length). The compressive strain ε is defined as the change in the length relative to the initial length of the gel specimen, i.e., $\varepsilon = 1 - \lambda$. Cyclic compression tests were conducted at a constant cross-head speed of 1 mm·$\min^{-1}$. The gel samples were first compressed up to a maximum strain λ_{max}, followed by retraction to zero relaxation force. After waiting for 1 min at zero relaxation force, the test was repeated four times with a fixed maximum strain as well as with increasing this strain. For reproducibility, at least five samples were measured for each gel and the results were averaged.

3. Results and discussion

3.1. HA hydrogels

HA hydrogels were prepared in aqueous NaOH solutions at 50 °C in the presence of EGDE cross-linker. The selection of NaOH solutions as the solvent to conduct the cross-linking reactions is due to the fact that the intramolecular hydrogen bonds in HA molecules are easily disrupted at high pH values [41], thereby providing a more flexible HA chain conformation and easier solubility in water. Increasing chain flexibility of HA in alkaline solutions will also promote the cross-linking reactions between its functional groups via the epoxy groups of EGDE. Preliminary experiments were carried out to optimize the concentrations of NaOH (C_{NaOH}) and HA (C_{HA}) during the gel formation. At $C_{NaOH} < 1$ w/v%, HA could not be completely dissolved in aqueous solutions while at higher NaOH concentrations (≥2 w/v%), the solution viscosity of HA and the elastic modulus G' of the resulting hydrogels drastically decreased indicating hydrolytic degradation of HA [41]. Moreover, at $C_{HA} < 8$ w/v%, weak hydrogels with an elastic modulus below 1 kPa were obtained in 1 w/v% NaOH solutions, while, at or above 10 w/v% HA, the preparation of a homogeneous HA solution was difficult due to the high solution viscosity. In the following, we present our results obtained in a 1 w/v% NaOH solution containing 8 w/v% HA and various amounts of the cross-linker EGDE. Rheological measurements conducted on 8 w/v% HA solution in 1 w/v% NaOH before the addition of the cross-linker showed a decrease in the solution viscosity and elastic modulus G' with increasing time or with increasing temperature (Figs. S1, S2). This behavior of alkaline HA solutions has been reported before [41], and it originates from the decrease of the size of HA molecules due to the disruption of intermolecular hydrogen bonds and/or from the degradation of HA backbone resulting in a decrease of the molecular weight.

We first monitored the gelation reactions by dynamic rheological measurements in order to follow the gradual formation of the three-dimensional HA network. Typical gelation profiles of 8 w/v% HA solutions at 50 °C and at four different cross-linker contents are shown in Fig. 1a where the elastic modulus G' and the loss factor tan δ are plotted against the reaction time. During the reactions, the elastic modulus G' increases rapidly while *tan* δ decreases and then, they approach plateau values after about 3 h. The higher the EGDE content, the higher the elastic modulus G', and the lower the loss factor *tan* δ indicating that increasing cross-linker content decreases the viscous, energy dissipating properties of HA hydrogels. To estimate the limiting modulus G'_∞ of the hydrogels, the experimental G' vs gelation time data were fitted to the equation [42–44]:

$$G'(t) \quad = \quad G'_\infty \frac{t^n}{t^n \ + \ \theta^n} \tag{1}$$

where θ is the half-gelation time at which the modulus G' becomes equal to $G'_\infty/2$, and the exponent n relates to the slope P at θ by:

$$P \quad = \quad \frac{n\, G'_\infty}{4\,\theta} \tag{1a}$$

The solid red curves in Fig. 1a showing the best fits to the experimental data indicate that Eq. 1 well simulates the gelation process of HA solutions. Gelation reactions conducted at eight different cross-linker concentrations between 0.95 and 22.4 w/v% EGDE revealed that both the half-gelation time θ and the coefficient n are almost independent on the EGDE content and they remain at 143 ± 38 min and 1.6 ± 0.3, respectively. This indicates that the cross-linking reactions are not accelerated with increasing EGDE concentration. In contrast, the slope P at the half-gelation time θ increased from 2 to 140 kPa·$\min^{-1}$ indicating formation of a larger number of intermolecular cross-links as the EGDE content is increased. The limiting values of G'_∞ obtained from the fits are shown in Fig. 1b together with the loss factor tan δ after a reaction time of 3 h both plotted against the EGDE concentration. HA hydrogels with an elastic modulus between 10^{-1} and 10^1 kPa could be obtained by tuning the cross-linker concentration. Moreover, the hydrogels exhibit a loss factor between 0.07 and 0.7, i.e., they belong to the category of weak gels [45].

After a reaction time of 4 h, dynamic frequency-sweep tests were carried out to explore the internal dynamics of HA hydrogels. Fig. 2a–e show the frequency dependencies of G' (filled symbols) and the viscous modulus G'' (open symbols) at a strain amplitude $\gamma_o = 0.01$ for the hydrogels formed at various EGDE contents. At the lowest cross-linker content of 0.95 w/v% EGDE (Fig. 2a), both G' and G'' increase with frequency similar to the semi-dilute polymer solutions. However, unlike these solutions, the present system exhibits an elastic character

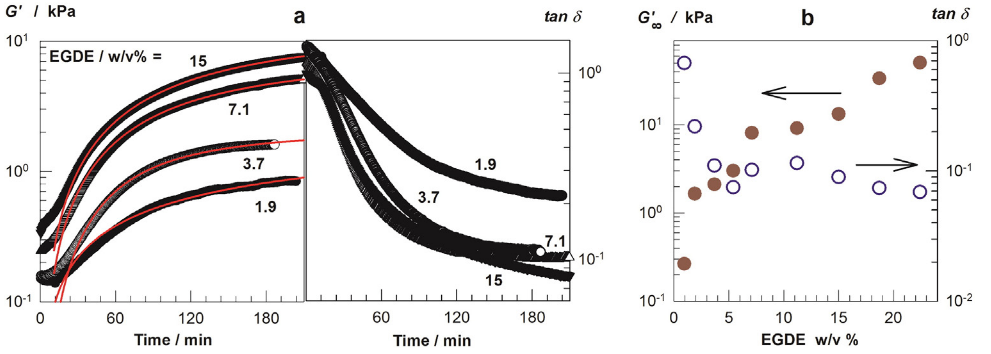

Fig. 1. Rheological monitoring of HA gelation. (a) Elastic modulus G' (left) and the loss factor $tan\ \delta$ (right) of the reaction system shown as a function of the reaction time. $\omega = 6.3$ rad.s^{-1}. $\gamma_o = 0.01$. Temperature = 50 °C. EGDE concentrations are indicated. The solid curves were calculated using Eq. 1. (b) The limiting elastic modulus G_∞' (filled symbols) and $tan\ \delta$ after a reaction time of 3 h (open symbols) plotted against EGDE %.

($G' > G''$) at low frequencies and a predominantly viscous character above the crossover frequency of 20 rad^{-1} at which G' and G'' intersect. This unusual behavior was observed before in aqueous solutions of sodium alginate - poly(N-isopropylacrylamide) (PNIPA) [46], HA-graft-PNIPA [47], and methyl cellulose [48]. We attribute this feature to the intermolecular hydrogen bonds between HA molecules acting as physical cross-links and thus, contributing to the elasticity of the hydrogel at a low frequency. Increasing frequency gradually breaks H-bonds so that the weak gel transforms to a viscous solution. As the cross-linker content is increased, the crossover frequency shifts outside of the experimental window indicating that the effect of chemical EGDE links dominate over the physical cross-links (Fig. 2a–e). However, the viscous modulus G'' still rises with frequency implying increasing extent of energy dissipation due to the rearrangement of HA molecules leading to their sliding past each other at short experimental time scales. Fig. 2 also shows that, at 3.7 w/v% EGDE, a plateau-like behavior appears in the low-frequency range, whereas the height of the plateau increases and its width expands as EGDE concentration is further increased. For instance, the plateau elastic modulus increases from 1.6 to 24.5 kPa with increasing EGDE content from 3.7 to 22.4 w/v% indicating increasing elastic response of the hydrogels.

After a gelation time of 4 h, HA hydrogels were subjected to swelling and mechanical measurements. The hydrogels formed below 2 w/v% EGDE were soluble in water while those formed at or above 3.7 w/v% EGDE were insoluble with a gel fraction W_g above 0.90 and contained 97–99% water (Table S1). Since the molecular weights of the cross-linker EGDE and the disaccharide repeat units of HA are 174.2 and 416 g·mol^{-1}, respectively, and HA concentration at gelation was fixed at 8 w/v%, a conversion factor of 0.15 converts the EGDE concentration (in w/v%) to the molar ratio of epoxide and hydroxide groups. Thus, the threshold concentration of 3.7 w/v% EGDE corresponds to the presence of about 0.56 epoxides per OH group, or 2.2 mol of epoxide groups per disaccharide repeat unit of HA molecules. Assuming that each epoxide group forms elastically effective cross-links, this molar ratio would lead to a ladder-like highly cross-linked HA structure with a modulus in the MPa range. Thus, a large fraction of EGDE in the gelation solution seems to be wasted in side reactions, such as the reaction of the epoxides with water, and/or is attached to HA only with its one end while the other end reacts with water.

All HA hydrogels described above were prepared by conducting the cross-linking reactions at 50 °C. Because HA may degrade at an elevated temperature, we repeated the gelation reactions at 25 °C. However, the reactions were too slow to monitor the gelation process by dynamic rheological measurements. Gravimetric tests conducted at or above 1.9 w/v% EGDE revealed that a gel fraction W_g above 0.90 could only be obtained by increasing the gelation time to 4 days (Table S1). The hydrogels formed both at 50 and 25 °C were subjected to swelling measurements in water. Filled circles in Fig. 3a & b show the relative swelling ratio m_{rel} (with respect to the as-prepared state) of HA hydrogels formed at 50 and 25 °C, respectively, plotted against their EGDE contents. For comparison, m_{rel} values of GMHA hydrogels reported before are also shown in Fig. 3a by the open symbols plotted against the methacrylation degree (DM) of GMHA [32]. m_{rel} of HA hydrogels is a decreasing function of the cross-linker content and varies between 2 and 123, corresponding to the equilibrium swelling ratio with respect to dry state of 25-1540. This high degree of swelling is a consequence of the osmotic pressure exerted by the counterions of cross-linked HA molecules, similar to the synthetic polyelectrolyte hydrogels [11]. The hydrogels formed at 25 °C exhibit a slightly lesser degree of swelling in water as compared to those formed at 50 °C. Another point is that HA hydrogels swell much more than those prepared from GMHA exhibiting relative swelling ratios m_{rel} between 3 and 4.5. This reveals a reduction in the hydrophilicity of native HA upon its modification with methacrylate groups.

Mechanical properties of HA hydrogels equilibrium swollen in water were investigated by uniaxial compression tests. Fig. 3c represents compressive stress-strain curves of the gel samples formed at 50 °C and at various EGDE contents, where the nominal stress σ_{nom} is plotted against the strain ε. In Fig. 3d & e, the Young's modulus E, fracture stress σ_f and fracture strain ε_f of the hydrogels formed at 50 °C and 25 °C,

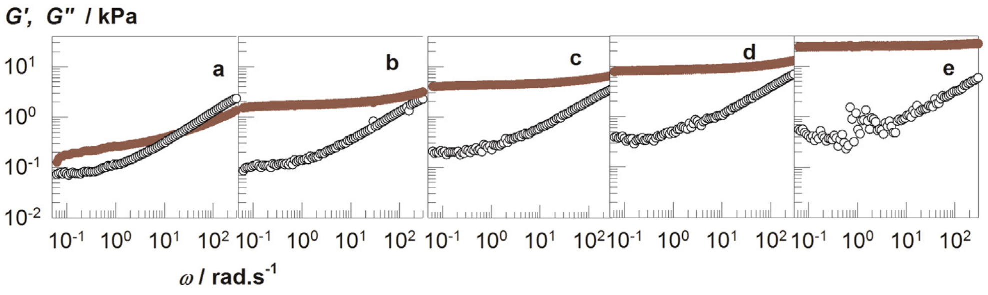

Fig. 2. G' (filled symbols) and G'' (open symbols) of HA hydrogels at 25 °C shown as a function of the frequency ω measured after a gelation time of 4 h. $\gamma_o = 0.01$. EGDE = 0.95 (a), 3.7 (b), 7.1 (c), 15.0 (d), and 22.4 w/v% (e).

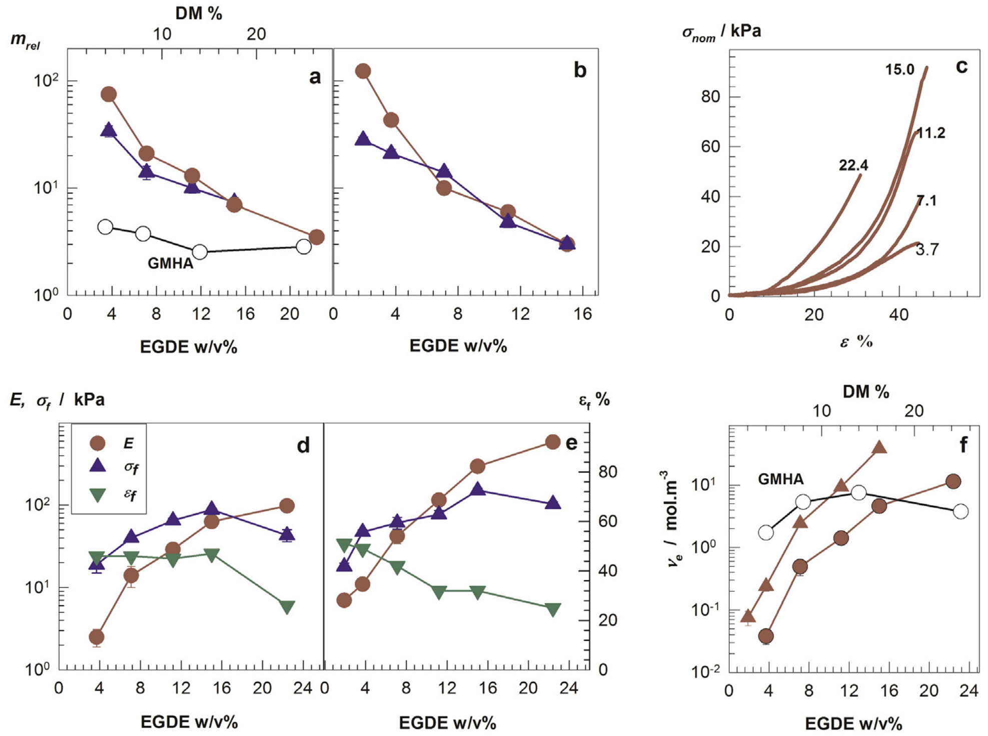

Fig. 3. Swelling behavior and mechanical properties of HA hydrogels. (a, b) Relative swelling ratio m_{rel} of HA hydrogels formed at 50 °C (a) and 25 °C (b) in water (filled circles) and in aqueous 30% DMA solution (filled triangles) plotted against EGDE%. For comparison, m_{rel} values of GMHA hydrogels reported before are also shown in Fig. 3a by the open symbols plotted against the methacrylation degree (DM) of GMHA [32]. (c) Typical stress-strain curves of HA hydrogels formed at 50 °C under compression as the dependences of nominal stress σ_{nom} on the strain ε. EGDE contents (in w/v%) are indicated. (d, e) Young's modulus E, fracture stress σ_f and fracture strain ε_f plotted against the EGDE content for the hydrogels formed at 50 °C (d) and 25 °C (e). (f) The cross-link density ν_e of HA hydrogels formed at 50 °C (filled circles) and 25 °C (filled triangles) plotted against EGDE %. Open symbols represent ν_e of GMHA hydrogels plotted against DM% of GMHA [32].

respectively, are plotted against the EGDE content. Depending on the cross-linker content and gelation temperature, Young's modulus E of the hydrogels varies one to two orders of magnitude, i.e., between 3 and 590 kPa. For a tetrafunctional phantom network of Gaussian chains, the Young's modulus E is related to the elastically effective cross-link density ν_e (number of network chains per unit volume of swollen gel) by [49,50]:

$$E = 1.5\nu_e RT(m_{rel})^{2/3} \tag{2}$$

where R is the gas constant and T is the absolute temperature. Note that Eq. (2) assumes that the weight swelling ratio m_{rel} is equal to the volume swelling ratio. In Fig. 3f, the cross-link density ν_e of HA hydrogels is shown as a function of the EGDE content. For comparison, ν_e of GMHA hydrogels is also plotted against DM% [32]. In accord with the lower swelling capacity of HA hydrogels formed at 25 °C, their modulus E and cross-link density ν_e are larger than those formed at 50 °C indicating increasing cross-linking efficiency by reducing the gelation temperature. The decrease of the cross-linking efficiency with rising temperature is attributed to the partial degradation of HA molecules producing shorter primary chains. Moreover, when comparing the swelling ratios of GMHA and HA hydrogels having similar cross-link densities, the former hydrogels exhibit a lower degree of swelling in water supporting the fact that the methacrylation makes HA less hydrophilic as compared to native HA. We have to note that because the cross-link density ν_e of the hydrogels calculated using Eq. (2) bases on the swollen gel volume, its value is affected by the swelling degree of the hydrogels. However, calculation of the cross-link densities based on dry polymer lead to the similar trends as mentioned above (Fig. S3).

The results in Fig. 3d & e also show that all HA hydrogels rupture when compressed to 25–51% strain under 20–150 kPa stresses. Thus, they are brittle hydrogels similar to the chemically cross-linked synthetic hydrogels [51], indicating that the viscoelastic energy dissipation of HA molecules under stress does not contribute much to their mechanical performances.

3.2. Double-network HA hydrogels

As mentioned in the previous section, HA hydrogels exhibit a larger degree of swelling as compared to those obtained from GMHA macromers. This suggests that a larger amount of a ductile component could be introduced during double-networking of HA hydrogels leading to double-network (DN) hydrogels with better mechanical properties as compared to those produced from GMHA macromers [33,52]. We prepared DN hydrogels by swelling HA hydrogels, taken as the first-network, in *N*,*N*-dimethylacrylamide (DMA) solutions containing a small amount of BAAm cross-linker, and then photopolymerizing DMA to form a loosely cross-linked poly(*N*,*N*-dimethylacrylamide) (PDMA) second network. The filled triangles in Fig. 3a & b show the swelling ratio m_{rel} of HA hydrogels formed at 50 and 25 °C, respectively, in aqueous 30 w/v% DMA solutions plotted against the EGDE content. Although a slight reduction in the swelling degree m_{rel} of the hydrogels in the DMA solution is observable as compared to their m_{rel} values in water, they still exhibit a high swelling ratio up to 40, which is one of the requirements for obtaining high strength DN hydrogels.

HA hydrogels swollen in 30 w/v% DMA solutions containing 0.05 and 0.10 mol% BAAm as the second-network cross-linker were subjected to photopolymerization using 2-oxoglutaric acid initiator. In this way, double-network hydrogels with a gel fraction W_g above 0.90 were obtained (Table S1). In equilibrium swollen state, they contained 84–94% water which decreased with increasing cross-linker content of the first-network hydrogel (Table S1). In the following DN hydrogels are denoted by DN-*x* where *x* is the mole percent of BAAm in the second monomer solution. Fig. 4 represents typical compressive stress-strain curves of SN hydrogels formed at 50 °C (dashed bold curves) and DN hydrogels (dash-dot-dot and solid curves) formed in 30 w/v% DMA

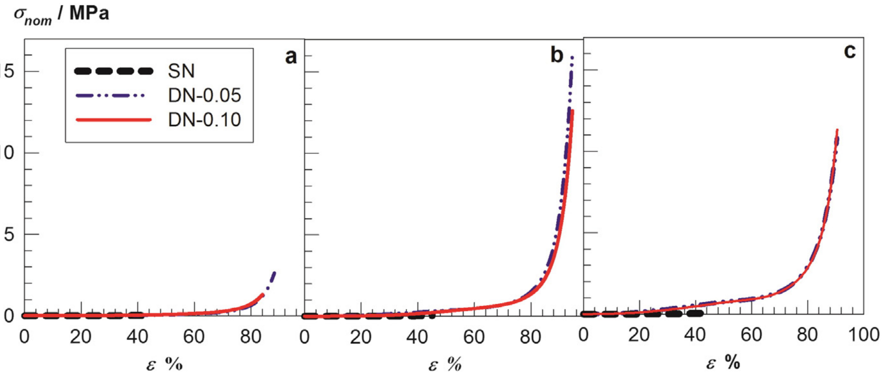

Fig. 4. Compressive stress-strain curves of SN hydrogels formed at 50 °C (dashed bold curves) and DN hydrogels (dash-dot-dot and solid curves). EGDE of the first-network HA hydrogel = 3.7 (a), 7.1 (b), and 11.2 w/v% (c). DN hydrogels were prepared in 30 w/v% DMA solutions containing 0.05 (dash-dot-dot curves) and 0.10 mol% BAAm cross-linker (solid curves).

solutions containing 0.05 and 0.10 mol% BAAm. EGDE content of the first network HA hydrogel is 3.7, 7.1, and 11.2 w/v% in Fig. 4a, b, and c, respectively. General trend is that the compressive stress required to deform the hydrogels increases from kPa to MPa scales after the double-networking process (Fig. 3c vs Fig. 4). Simultaneously, compression ratio at rupture increases from 26 to 47% to above 80% indicating toughening effect of the second PDMA network. It is also obvious that the EGDE content of the first HA network, that is, its cross-link density has a significant effect on the mechanical performance of DN hydrogels. We have to note that DN hydrogels were rather brittle in tensile tests with very low elongation at break. As a consequence, tensile tests could not be performed in a meaningful way.

In Fig. 5a & b, Young's modulus E, the fracture stress σ_f and strain at break ε_f of single-network HA (open symbols) and DN hydrogels (filled symbols) are plotted against EGDE concentration. The first-network HA hydrogels were prepared at 50 °C and 25 °C in (a) and (b), respectively. The modulus E of DN hydrogels is more than one order of magnitude greater than that of SN hydrogels and approaches to 1 MPa at high EGDE concentrations (Table S1). This increase in the modulus suggests the existence of physical and chemical cross-links between the first-

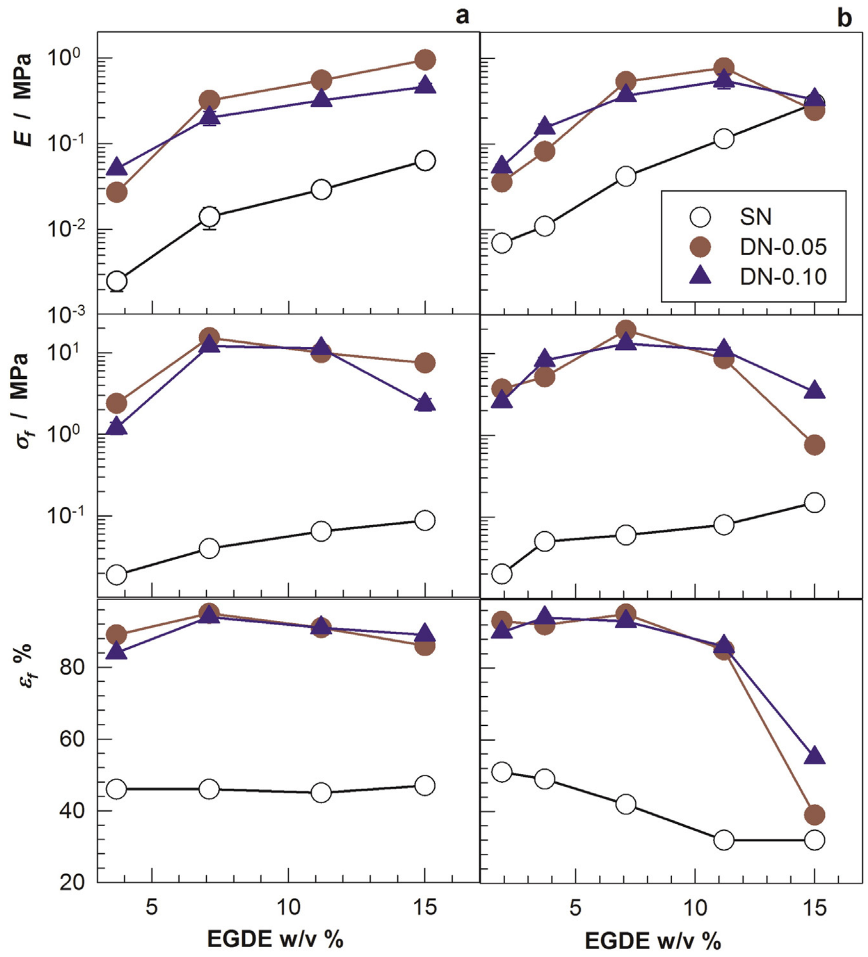

Fig. 5. Young's modulus E, the fracture stress σ_f and strain ε_f of SN (open symbols) and DN hydrogels (filled symbols) plotted against EGDE concentration. Preparation temperature of HA hydrogel = 50 °C (a) and 25 °C (b). Note that most of the error bars are smaller than the symbols.

and second-network components contributing to the rubber elasticity of DN hydrogels. The fracture stress σ_f and strain at break ε_f exhibit slight maxima at around 7 w/v% EGDE. The largest modulus and fracture stress of DN hydrogels thus obtained are 0.94 ± 0.13 MPa and 19.4 ± 0.9 MPa, respectively. These values are higher than those of DN hydrogels prepared from GMHA macromer exhibiting fracture stresses up to 5.2 and 12 MPa for 10 and 4% methacrylation degrees of HA, respectively [31,32]. Moreover, comparison of the mechanical characteristics of DN-0.05 and DN-0.10 hydrogels also indicates that the amount of the second-network cross-linker in this range does not have an effect on the mechanical properties of DN hydrogels.

To demonstrate the effect of the amount of the second PDMA ductile network on the mechanical performance of the hydrogels, we calculated the mass ratio w_{21} of PDMA to the HA first-network by

$$w_{21} = \frac{(m_{rel}-1)\,C_2}{C_1} \tag{3}$$

where m_{rel} is the swelling ratio of HA hydrogel in 30 w/v% DMA solution, C_1 and C_2 are the concentrations (in $\mathrm{g \cdot mL^{-1}}$) of HA and DMA in the preparation of the first- and double-network hydrogels, respectively. Note that Eq. (3) assumes that the densities of the hydrogels and DMA solution are equal to unity. Further, it neglects the exchange of water in the hydrogel with the external solution and thus, only consider monomer solution entering the gel phase during the swelling process to simulate real processes [52,53]. Because both C_1 and C_2 are fixed by the experiments at 0.08 and 0.30 $\mathrm{g \cdot mL^{-1}}$, respectively, the ratio w_{21} only depends on the swelling capacity of HA hydrogels in the DMA solution.

In Fig. 6a–c, the filled symbols represent the fracture stress σ_f, Young's modulus E, and fracture strain ε_f of all DN hydrogels plotted against w_{21} ratio. For comparison, the data for SN hydrogels ($w_{21} = 0$) are also shown in the figures by the open symbols. The results demonstrate that the w_{21} ratio is an effective parameter determining the mechanical properties of the hydrogels. The fracture stress σ_f of SN hydrogels formed at two different temperatures (25 and 50 °C) and at various cross-linker contents (between 1.9 and 22.4 w/v% EGDE) is between 20 and 150 kPa (open symbols in Fig. 6a). After double networking, σ_f rapidly increases with increasing w_{21} and attains a maximum value of 19.4 ± 0.9 MPa at $w_{21} = 49$. Further increase in w_{21} ratio again decreases the mechanical strength of the hydrogels up to 1.2 ± 0.2 MPa at $w_{21} = 126$. Because a very high w_{21} ratio requires a high swelling capacity and thus, a loosely cross-linked HA first-network, crack propagation cannot be prevented during deformation leading to worsening the mechanical performance of DN hydrogels. A similar trend is also observable in the variations of Young's modulus E and fracture strain ε_f of the hydrogels as a function of w_{21} ratio. (Fig. 6b & c). We should note that, in classical DN hydrogels prepared from poly(2-acrylamido-2-methylpropanesulfonic acid) (PAMPS) first-network and polyacrylamide second-network, the maximum enhancement in the compressive stress at break occurs when the molar ratio of the second to the first-network is around 20 corresponding to the weight ratio w_{21} of 7 [33]. This means that for the present HA/PDMA double-network system, a much larger amount of the ductile component PDMA ($w_{21} \cong 50$) should be introduced in the first network to achieve the maximum enhancement in the mechanical properties. This feature could be related to the presence of a lesser number of linkages between the 1st and 2nd networks. Previous work shows that the formation of mechanically strong DN hydrogels requires strong chain entanglements or covalent links between the 1st and 2nd polymer networks [32,52,54]. In the case of SN hydrogels formed by vinyl–divinyl monomer copolymerization such as PAMPS hydrogels, the initiator molecules remaining in the first network as well as the pendant vinyl groups of divinyl monomer units are able to form potential cross-linking points between 1st and 2nd networks [54]. However, for the present DN system, HA chains are unable to covalently link the first to the second

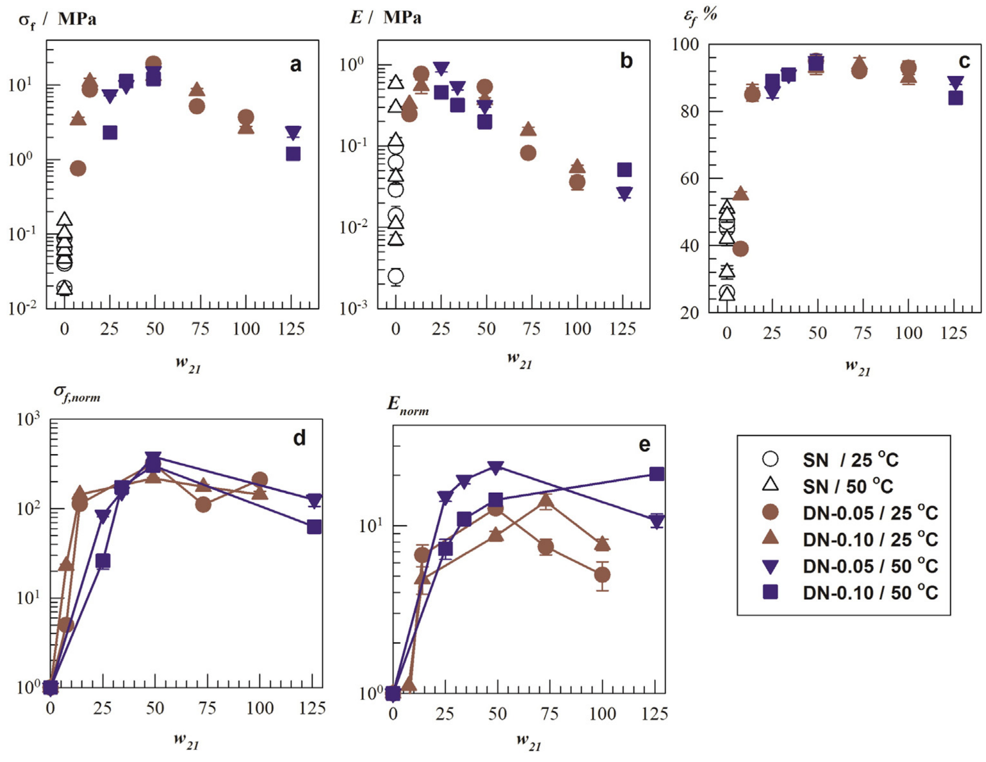

Fig. 6. Mechanical properties of DN hydrogels as a function of the w_{21} ratio. (a-c) The fracture stress σ_f (a), Young's modulus E (b), and strain at break ε_f (c) of SN (open symbols) and DN hydrogels (filled symbols) plotted against the w_{21} ratio. (d, e): Normalized fracture stress $\sigma_{f,norm}$ (d), and Young's modulus E_{norm} (e), of the hydrogels plotted against w_{21} ratio. Preparation temperature of HA hydrogel = 25 °C (dark red) and 50 °C (blue). Note that most of the error bars are smaller than the symbols. (For interpretation of the references to colour in this figure legend, the reader is referred to the web version of this article.)

network so that a larger amount of PDMA is required to create strong chain entanglements.

We have to mention that the modulus E of SN hydrogels increases from 3 kPa to 586 ± 62 kPa with increasing EGDE content and thus approaches to the highest modulus of DN hydrogels (open symbols in Fig. 6b). However, high-modulus SN hydrogels were very brittle and ruptured at very low compression ratios. For instance, HA hydrogels with a modulus $E = 586$ kPa formed at 25 °C and at 22.4 w/v% EGDE content already fractured during the formation of their DN hydrogels. In contrast, double-networking process increases both the modulus, i.e., effective cross-link density of the hydrogels and the mechanical strength. The degree of improvement in the mechanical properties of HA hydrogels is illustrated in Fig. 6d & e where the fracture stress $\sigma_{f,norm}$ (d), and Young's modulus E_{norm}, normalized with respect to those of the first-network hydrogels, are plotted against the w_{21} ratio. It is seen that up to 380–fold increase in the fracture stress and 23–fold increase in the modulus were achieved by applying DN approach.

We attribute the improvement in the mechanical properties of HA hydrogels after double networking to the higher cross-link density of the first HA network as compared to the second PDMA network. Because the short HA network chains attain a highly stretched conformation upon swelling in the second monomer solution, the resulting DN hydrogel consists of highly stretched HA and randomly coiled PDMA network chains. Thus, the first HA network internally fractures under low stresses by dissipating energy while the second PDMA network keeps the macroscopic gel sample together and prevents macro-crack formation. We have to mention that the mass ratio w_{21} of the second to the first-network achieved using HA hydrogels is much higher as compared to that obtained using GMHA hydrogels ($w_{21} = 126$ vs 29) [32]. This also contributes to the mechanical strength of the present hydrogels. Thus, the internal fracture of HA network together with the high mass ratio of the second to the first-network components seem to be responsible for the extraordinary mechanical properties of the hydrogels. To demonstrate this internal fracture, a series of cyclic compression experiments were performed on DN hydrogels. Fig. 7a represents stress-strain curves of a DN hydrogel formed at $w_{21} = 49$ from a compression test composed of five successive cycles up to a maximum compression of 80% ($\lambda_{max} = 0.20$). The results are presented as the dependence of the true stress σ_{true} ($= \lambda\sigma_{nom}$) on the compression ratio λ (deformed length/initial length) The loading and unloading curves are indicated by up and down arrows, respectively. The loading path of the first compressive cycle conducted on a fresh hydrogel sample differs from the unloading path indicating damage in the sample and dissipation of energy. The hysteresis energy U_{hys} in this cycle, calculated from the area between the loading and unloading curves, is 220 ± 20 $\text{kJ} \cdot \text{m}^{-3}$. However, the following loading/unloading cycles are almost elastic with a small hysteresis area ($U_{hys} = 18 \pm 1\ \text{kJ} \cdot \text{m}^{-3}$), and they all closely follow the path of the first unloading. The results indicate the occurrence of an irrecoverable internal damage during the first compression of the gel sample.

The hysteresis energy U_{hys} can be interpreted as the energy released due to fracture of the first-network during deformation. This fracture can take place in EGDE cross-links as well as in the glycosidic linkages of HA chains. In both cases, breaking of C—O bonds results in a decrease in the effective cross-link density ν_e of the first-network. Thus, U_{hys} is equal to the product of C—O bond energy U_{xl} and the total number of effective cross-links broken down during the compression cycle [36,55], i.e.

$$U_{hys} = U_{xl}\ (\nu_e\ f_\nu) \tag{4}$$

where f_ν is the fraction of effective cross-links broken during the mechanical cycles. Since C—O bond energy U_{xl} is 360 $\text{kJ} \cdot \text{mol}^{-1}$ and $\nu_e = 304 \pm 60\ \text{mol} \cdot \text{m}^{-3}$ (Fig. 3f), one may solve Eq. 4 for the fraction f_ν of effective cross-links broken during the mechanical cycles in Fig. 7a. Calculations show that 25 ± 4% of the cross-links are irreversible broken during the first loading while 2% additional bonds are broken in each of the following loadings.

The cyclic tests conducted up to a fixed maximum strain of 80% were repeated with a virgin gel sample with increasing maximum strain from 40 to 80% in five successive cycles ($\lambda_{max} = 0.6$ to 0.2). The results are shown in Fig. 7b were the loading and unloading curves are presented by solid and dashed lines, respectively. After the first compressive cycle, each successive loading curve is composed of two regions, as also illustrated in Fig. 7c for the cycle 5 ($\lambda_{max,\,5} = 0.20$). The first region is elastic and it follows the path of the unloading curve of the previous cycle while the second region creates an additional damage by continuing the loading curve of the previous cycle. The transition from the first (elastic) to the second (damage) region always occurred at the maximum strain of the previous cycle. Thus, due to the irreversible damage done during the previous cycle, additional damage only occurs at a higher maximum strain. In Fig. 7d, the fraction f_ν of cross-links broken are plotted against the maximum strain λ_{max}. The open triangle in the figure represents the fraction f_ν of broken cross-links during one-step cycle up to $\lambda_{max} = 0.20$ obtained from Fig. 7a. Increasing maximum strain also increases the number of broken bonds in the first network. Moreover, compression of the hydrogel sample with successive five-step cycles with increasing maximum strain up to 80% results in the same number of broken bonds as in a one-step cycle with a maximum strain of 80%. This indicates that the extent of damage in the hydrogels

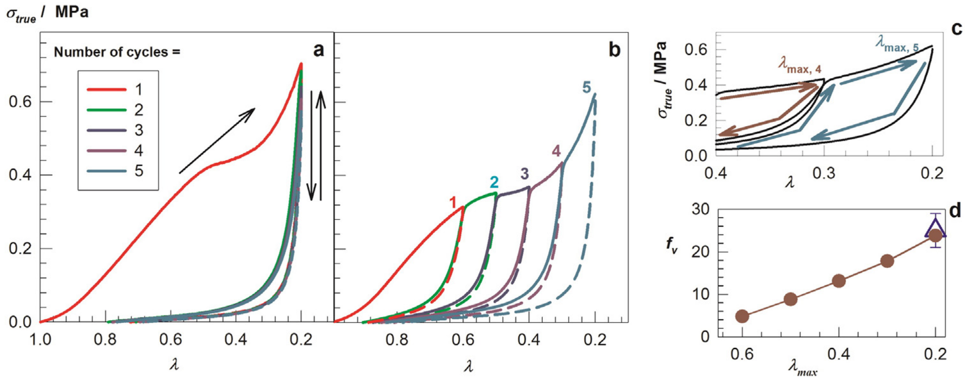

Fig. 7. Cyclic mechanical tests of DN hydrogels. (a, b) Typical stress-strain curves of a DN hydrogel from a compression test composed of five successive cycles. The true stress σ_{true} is plotted against the compression ratio λ (deformed length/initial length). The maximum compression was fixed at 80% ($\lambda_{max} = 0.20$) in (a) while in (b), it was stepwise increased from 40 to 80% in successive cycles ($\lambda_{max} = 0.60$ to 0.20). EGDE = 7.1 w/v%. BAAm = 0.05 w/v%. $w_{21} = 49$. The up and down arrows in (a) indicate loading and unloading curves, respectively. For clarity, loading and unloading curves are shown by the solid and dashed curves, respectively. (c) A zoom-in to Fig. 7b to highlight the damage and elastic regions of the 5th cycle. (d) The fraction f_ν of EGDE cross-links broken during the mechanical cycles with increasing maximum compression from 40 to 80% ($\lambda_{max} = 0.60$ to 0.20). The open triangle represents the fraction f_ν during a one-step mechanical cycle up to 80% compression.

is path-independent and it only depends on the maximum deformation ratio of the network chains.

4. Conclusions

We presented a two-step procedure for the preparation of high-strength HA hydrogels starting from native HA. In the first step, HA was cross-linked in aqueous solutions using EGDE cross-linker under various experimental conditions. It was found that EGDE-cross-linked HA hydrogels containing 97–99% water are fragile, and rupture when compressed to 25–51% strain under 0.02–0.15 MPa stresses. By applying the double-network approach in the second step, we were able to generate high strength HA/PDMA double-network hydrogels containing 84–94% water. Tuning the ratio of the network components could result in hydrogels exhibiting a compressive modulus of 0.9 MPa that sustain 19.4 MPa compressive stresses, which are much larger than those reported before for the hydrogels derived from the methacrylated HA macromers. Cyclic mechanical test results indicate that an irrecoverable internal damage occurs in DN hydrogels at compressions as low as 40% at which single-network HA hydrogels visibly rupture. The results indicate that the lightly cross-linked PDMA second-network holds the macroscopic gel sample together by hindering the micro-crack propagation to a macroscopic scale, while the gel sample internally fractures. This internal fracture of HA first-network together with the high mass ratio of the second to the first-network components are responsible for the extraordinary mechanical properties of the hydrogels. HA-based hydrogels presented here with good mechanical properties and high water contents are promising materials to make use the characteristics of HA in stress-bearing biomedical applications.

Acknowledgements

This work was supported by the Scientific and Technical Research Council of Turkey (TUBITAK), KBAG 114Z312. O.O. thanks the Turkish Academy of Sciences (TUBA) for the partial support.

References

[1] J.R. Fraser, T.C. Laurent, U.B. Laurent, Hyaluronan: its nature, distribution, functions and turnover, J. Intern. Med. 242 (1997) 27–33.
[2] W.Y. Chen, G. Abatangelo, Functions of hyaluronan in wound repair, Wound Repair Regen. 7 (1999) 79–89.
[3] L.J. Lapcík, L. Lapcík, S.D. Smedt, J. Demeester, P. Chabracek, Hyaluronan: preparation, structure, properties, and applications, Chem. Rev. 98 (1998) 2663–2684.
[4] G. Kogan, L. Soltes, R. Stern, P. Gemeiner, Hyaluronic acid: a natural biopolymer with a broad range of biomedical and industrial applications, Biotechnol. Lett. 29 (2007) 17–25.
[5] J. Necas, L. Bartosikova, R. Brauner, J. Kolar, Hyaluronic acid (hyaluronan): a review, Vet. Med. 53 (2008) 397–411.
[6] E. Neovius, M. Lemberger, A.C. Docherty Skogh, J. Hilborn, T. Engstrand, Alveolar bone healing accompanied by severe swelling in cleft children treated with bone morphogenetic protein-2 delivered by hydrogel, J. Plast. Reconstr. Aesthet. Surg. 66 (2013) 37–42.
[7] X. Xu, A.K. Jha, D.A. Harrington, M.C. Farach-Carson, X. Jia, Hyaluronic acid-based hydrogels: from a natural polysaccharide to complex networks, Soft Matter 8 (2012) 3280–3294.
[8] T. Luan, L. Wu, H. Zhang, Y. Wang, A study on the nature of intermolecular links in the cryotropic weak gels of hyaluronan, Carbohydr. Polym. 87 (2012) 2076–2085.
[9] M.N. Collins, C. Birkinshaw, Comparison of the effectiveness of four different crosslinking agents with hyaluronic acid hydrogel films for tissue-culture applications, J. Appl. Polym. Sci. 104 (2007) 3183–3191.
[10] M.N. Collins, C. Birkinshaw, Hyaluronic acid based scaffolds for tissue engineering - a review, Carbohydr. Polym. 92 (2013) 1262–1279.
[11] F. Horkay, A.-M. Hecht, E. Geissler, Similarities between polyelectrolyte gels and biopolymer solutions, J. Polym. Sci. B Polym. Phys. 44 (2006) 3679–3686.
[12] K. Tomihata, Y. Ikada, Preparation of cross-linked hyaluronic acid films of low water content, Biomaterials 18 (1977) 189–195.
[13] T. Segura, B.C. Anderson, P.H. Chung, R.E. Webber, K.R. Shull, L.D. Shea, Crosslinked hyaluronic acid hydrogels: a strategy to functionalize and pattern, Biomaterials 26 (2005) 359–371.
[14] H.-D. Hwang, H.-J. Cho, P. Balakrishnan, C.-W. Chung, I.-S. Yoon, Y.-K. Oh, Y. Byun, D.-D. Kim, Cross-linked hyaluronic acid-based flexible cell delivery system: application for chondrogenic differentiation, Colloids Surf. B: Biointerfaces 91 (2012) 106–113.
[15] H.J. Kim, K.K. Kim, I.K. Park, B.S. Choi, J.H. Kim, M.S. Kim, Hybrid scaffolds composed of hyaluronic acid and collagen for cartilage regeneration, J. Tissue Eng. Regen. Med. 9 (2012) 57–62.
[16] H.R. Brown, A model of the fracture of double network gels, Macromolecules 40 (2007) 3815–3818.
[17] S. Abdurrahmanoglu, V. Can, O. Okay, Design of high-toughness polyacrylamide hydrogels by hydrophobic modification, Polymer 50 (2009) 5449–5455.
[18] A. Strom, A. Larsson, O. Okay, Preparation and physical properties of hyaluronic acid-based cryogels, J. Appl. Polym. Sci. 132 (2015) 42194.
[19] C. Oelschlaeger, F. Bossler, N. Willenbacher, Synthesis, structural and micromechanical properties of 3D hyaluronic acid-based cryogel scaffolds, Biomacromolecules 17 (2016) 580–589.
[20] O. Okay, V.I. Lozinsky, Synthesis and structure–property relationships of cryogels, Adv. Polym. Sci. 263 (2014) 103–157.
[21] J.B. Leach, K.A. Bivens, C.W. Patrick, C.E. Schnidt, Photocrosslinked hyaluronic acid hydrogels: natural, biodegradable tissue engineering scaffolds, Biotechnol. Bioeng. 82 (2003) 578–589.
[22] S.S. Prado, J.M. Weaver, B.J. Love, Gelation of photopolymerized hyaluronic acid grafted with glycidyl methacrylate, Mater. Sci. Eng. C 31 (2011) 1767–1771.
[23] S. Ibrahim, C.R. Kothapalli, Q.K. Kang, A. Ramamurthi, Characterization of glycidyl methacrylate – crosslinked hyaluronan hydrogel scaffolds incorporating elastogenic hyaluronan oligomers, Acta Biomater. 7 (2011) 653–665.
[24] X.Z. Shu, Y. Liu, Y. Luo, M.C. Roberts, G.D. Prestwich, Disulfide cross-linked hyaluronan hydrogels, Biomacromolecules 3 (2002) 1304–1311.
[25] K. Ghosh, X. Zheng Shu, R. Mou, J. Lombardi, G.D. Prestwich, M.H. Rafailovich, R.A.F. Clark, Rheological characterization of in situ cross-linkable hyaluronan hydrogels, Biomacromolecules 6 (2005) 2857–2865.
[26] A.F. Jeffery, M.A. Churchward, V.K. Mushahwar, K.G. Todd, A.L. Elias, Hyaluronic acid-based 3D culture model for in vitro testing of electrode biocompatibility, Biomacromolecules 15 (2014) 2157–2165.
[27] X. Jia, J.A. Burdick, J. Kobler, R.J. Clifton, J.J. Rosowski, S.M. Zeitels, R. Langer, Synthesis and characterization of in situ cross-linkable hyaluronic acid-based hydrogels with potential application for vocal fold regeneration, Macromolecules 37 (2004) 3239–3248.
[28] R. Elia, D.R. Newhide, P.D. Pedevillano, G.R. Reiss, M.A. Firpo, E.W. Hsu, D.L. Kaplan, G.D. Prestwich, R.A. Peattie, Silk–hyaluronan-based composite hydrogels: a novel, securable vehicle for drug delivery, J. Biomater. Appl. 27 (2011) 749–762.
[29] K.H. Chang, H.T. Liao, J.P. Chen, Preparation and characterization of gelatin/hyaluronic acid cryogels for adipose tissue engineering: in vitro and in vivo studies, Acta Biomater. 9 (2013) 9012–9026.
[30] C. Foss, E. Merzari, C. Migliaresi, A. Motta, Silk fibroin/hyaluronic acid 3D matrices for cartilage tissue engineering, Biomacromolecules 14 (2013) 38–47.
[31] L. Weng, A. Gouldstone, Y. Wu, W. Chen, Mechanically strong double network photocrosslinked hydrogels from N, N-dimethylacrylamide and glycidyl methacrylated hyaluronan, Biomaterials 29 (2008) 2153–2163.
[32] B. Tavsanli, V. Can, O. Okay, Mechanically strong triple network hydrogels based on hyaluronan and poly(*N*,*N*-dimethylacrylamide), Soft Matter 11 (2015) 8517–8524.
[33] J.P. Gong, Y. Katsuyama, T. Kurokawa, Y. Osada, Double-network hydrogels with extremely high mechanical strength, Adv. Mater. 15 (2003) 1155–1158.
[34] Y. Tanaka, J.P. Gong, Y. Osada, Novel hydrogels with excellent mechanical performance, Prog. Polym. Sci. 30 (2005) 1–9.
[35] M.A. Haque, T. Kurokawa, J.P. Gong, Super tough double network hydrogels and their application as biomaterials, Polymer 53 (2012) 1805–1822.
[36] R.E. Webber, C. Creton, H.R. Brown, J.P. Gong, Large strain hysteresis and Mullins effect of tough double-network hydrogels, Macromolecules 40 (2007) 2919–2927.
[37] T. Nakajima, T. Kurokawa, S. Ahmed, W. Wu, J.P. Gong, Characterization of internal fracture process of double network hydrogels under uniaxial elongation, Soft Matter 9 (2013) 1955–1966.
[38] X. Lu, Y. Xu, C. Zheng, G. Zhang, Z. Su, Ethylene glycol diglycidyl ether as a protein cross-linker: a case study for cross-linking of hemoglobin, J. Chem. Technol. Biotechnol. 81 (2006) 767–775.
[39] F. Topuz, O. Okay, Rheological behavior of responsive DNA hydrogels, Macromolecules 41 (2008) 8847–8854.
[40] I. Karakutuk, F. Ak, O. Okay, Diepoxide-triggered conformational transition of silk fibroin: formation of hydrogels, Biomacromolecules 13 (2012) 1122–1128.
[41] M. Gatej, M. Popa, Rinaudo, Role of the pH on hyaluronan behavior in aqueous solution, Biomacromolecules 6 (2005) 61–67.
[42] D. Calvet, J.Y. Wong, S. Giasson, Rheological monitoring of polyacrylamide gelation: importance of cross-link density and temperature, Macromolecules 37 (2004) 7762–7771.
[43] J. Giraldo, N.M. Vivas, E. Vila, A. Badia, Assessing the (a)symmetry of concentration-effect curves: empirical versus mechanistic models, Pharmacol. Ther. 95 (2002) 21–45.
[44] O. Okay, W. Oppermann, Polyacrylamide - clay nanocomposite hydrogels: rheological and light scattering characterization, Macromolecules 40 (2007) 3378–3387.
[45] A.H. Clark, S.B. Ross-Murphy, Structural and mechanical properties of biopolymer gels, Adv. Polym. Sci. 83 (1987) 57–192.
[46] M. Teodorescu, M. Andrei, G. Turturică, P.O. Stănescu, A. Zaharia, A. Sârbu, Novel thermoreversible injectable hydrogel formulations based on sodium alginate and poly(*N*-isopropylacrylamide), Int. J. Polym. Mater. Polym. Biomater. 64 (2015) 763–771.
[47] M. D'Este, M. Alini, D. Eglin, Single step synthesis and characterization of thermoresponsive hyaluronan hydrogels, Carbohydr. Polym. 90 (2012) 1378–1385.
[48] M. Kundu, S. Mallapragada, R.C. Larock, P.P. Kundu, Rheological properties of methylcellulose aqueous gels under dynamic compression: frequency sweep and validity of scaling law, J. Appl. Polym. Sci. 117 (2010) 2436–2443.

[49] L.R.G. Treloar, The Physics of Rubber Elasticity, University Press, Oxford, 1975.
[50] P.J. Flory, Principles of Polymer Chemistry, Cornell University Press, Ithaca, NY, 1953.
[51] P. Calvert, Hydrogels for soft machines, Adv. Mater. 21 (2009) 743–756.
[52] A. Argun, V. Can, U. Altun, O. Okay, Non-ionic double and triple network hydrogels of high mechanical strength, Macromolecules 47 (2014) 6430–6440.
[53] N. Kayaman, O. Okay, B.M. Baysal, Swelling of polyacrylamide gels in aqueous solutions of ethylene glycol oligomers, Polym. Gels Networks 5 (1997) 339–356.
[54] T. Nakajima, H. Furukawa, Y. Tanaka, T. Kurokawa, Y. Osada, J.P. Gong, True chemical structure of double network hydrogels, Macromolecules 42 (2009) 2184–2189.
[55] G.J. Lake, A.G. Thomas, The strength of highly elastic materials, Proc. R. Soc. Lond. A 300 (1967) 108–119.